INTERNATIONAL JOURNAL OF OPTIMIZATION IN CIVIL ENGINEERING
Int. J. Optim. Civil Eng., 2022; 12(1):47-67

SEMI-ACTIVE NEURO-CONTROL FOR MINIMIZING SEISMIC RESPONSE OF BENCHMARK STRUCTURES

M. Payandeh-Sani and B. Ahmadi-Nedushan[*,†]

Department of Civil Engineering, Yazd University, Yazd, Iran

ABSTRACT

This article presents numerical studies on semi-active seismic response control of structures equipped with Magneto-Rheological (MR) dampers. A multi-layer artificial neural network (ANN) was employed to mitigate the influence of time delay, This ANN was trained using data from the El-Centro earthquake. The inputs of ANN are the seismic responses of the structure in the current step, and the outputs are the MR damper voltages in the current step. The required training data for the neural controller is generated using genetic algorithm (GA). Using the El-Centro earthquake data, GA calculates the optimal damper force at each time step. The optimal voltage is obtained using the inverse model of the Bouc-Wen based on the predicted force and the corresponding velocity of the MR damper. This data is stored and used to train a multi-layer perceptron neural network. The ANN is then employed as a controller in the structure. To evaluate the efficiency of the proposed method, three- story, seven- story and twenty-story structures with a different number of MR dampers were subjected to the Kobe, Northridge, and Hachinohe earthquakes. The maximum reduction in structural drifts in the three-story structure are 13.05%, 39.90%, 15.89%, and 8.21%, for the El-Centro, Hachinohe, Kobe, and Northridge earthquakes, respectively. As the control structure is using a pre-trained neural network, the computation load in the event of an earthquake is extremely low. Additionally, as the ANN is trained on seismic pre-step data to predict the damper's current voltage, the influence of time lag is also minimized.

Keywords: perceptron neural network; generalized regression neural network; genetic algorithm; semi-active control; MR damper.

Received: 14 November 2021; Accepted: 18 January 2022

1. INTRODUCTION

In the last two decades, semi-active vibration control of civil engineering structures has been

[*] Corresponding author: Department of Civil Engineering, Yazd University, Yazd, Iran
[†]E-mail address: behrooz.ahmadi@yazd.ac.ir (B. Ahmadi-Nedushan)

an active research discipline, and various methods have been proposed to reduce life-loss and significant damages to the structure. In this regard, numerous instruments and algorithms have been proposed. The control instruments and algorithms used in the structures can be classified into four categories: passive control [1-3], active control [4,5], semi-active control [6] and hybrid control [7]. Instruments used in the semi-active control do not require a significant amount of energy [6]. As a result, systems equipped with this control mechanism can be considered to be more stable. Among the instruments used for semi-active structural control, magneto-rheological dampers have attracted considerable attention in recent years. Utilizing these instruments can significantly reduce the structure's response to an earthquake and therefore, MR dampers can be considered as one of the reliable devices for semi-active control of structures. These dampers were first used in the national museum of science and innovation in Tokyo in 2001 [2]. MR dampers with a capacity of 30 tons were installed in the structure's fifth and seventh stories. Xu et al. used MR dampers to control a twelve-story structure using the El-Centro earthquake data [8]. The results indicated that the acceleration and displacement of the structure at different stories are significantly reduced. The resistant force exerted on the structure by these instruments is proportional to the relative velocity at the damper location and the instrument's input voltage.

Numerous mathematical models have been proposed to simulate the damper's behavior. Dominguez et al. proposed a bar element with node connections composed of five different materials to simulate the damper's dynamic behavior [9]. This model was used in the finite element model of a cantilever 3-D space truss structure with four bays exposed to different excitations. In addition, the Bingham model, the modified Bingham model, the Bing-Max model, the three-element model and the Bouc-Wen model are other numerical solutions to simulate the dampers' behavior [10]. Many algorithms have been proposed and implemented to control the structures in the semi-active control system. These techniques are classified into two categories: parametric [11] and numerical [12]. In the parametric method, the system's behavior is controlled using the mathematical equations of the system's control model. Parametric methods include second-order linear regulator [13], Gaussian second-order linear approach [14-16], and sliding mode control [17]. The second group are data-based models and does not require an explicit mathematical model.

Soft computing methods have been used in many applications for active and semi-active control of structures. The application of different types of neural networks [18, 19], fuzzy logic [20] and their combination in the fuzzy-neural algorithm [21] has been very effective in structural control systems. These algorithms can be used as controllers [22], structural behavior simulators [23] and MR damper modeling [24]. Neural networks are one of the most widely used soft computing methods across all fields of civil engineering and have been applied in various applications [25-30]. Using neural network as an analysis tool alleviates some of the computational load [25,26]. Additionally, neural networks are quite effective at forecasting the behavior of materials [27] and structural members [28]. ANNs have also been used successfully for real-time analysis of dam monitoring data [29, 30].

Due to the complexity of modeling structures' seismic behavior and the dampers used in structural control, ANNs have found many applications in the field of structural control. Ghabousi and Joghataie were pioneers in using neuro-controller in the field of structural control [31]. In their research, the ANNs were used for active control of a three-story

structure. The ANNs were trained so that the structure's behavior could be predicted in the next step. Bani Hani et al. have used ANNs for the semi-active control of structures [14]. The Gaussian second-order linear method was used to control the structure and calculate the appropriate control force. One of the challenges in using MR dampers is determining the optimum MR damper voltage according to the design criteria [32]. The wavelet neural network-based semi-active controller has been used successfully to provide the accurately computed input voltage of the MR dampers and to generate the optimal control force [33]. The parameters of ANN were optimized by a modified GA and the optimized ANN was used to control a nine-story benchmark structure. Bitaraf et al. applied a genetic-based fuzzy controller to determine the command voltage of the MR dampers [34]. A multi-objective GA is used to optimize the fuzzy logic controller rule-base to reduce the displacement and acceleration response of the considered structure. Zabihi et al. controlled a three-story structure using the Cuckoo-Fuzzy algorithm [35]. They suggested a novel evolutionary algorithm based on cuckoo search to determine the optimal location and number of dampers.

In structural control, time delay reduces the efficiency of the proposed methods [36]. Katebi et al. proposed a time-delay compensation method in coupled structures using the Newmark-beta formulation. Lyapunov's direct algorithm was used to determine the appropriate control force. Time delay always reduces the efficiency of the control systems. The present research offers a novel approach to overcome this deficiency. We propose using a neural network to predict the appropriate voltage of the dampers in the next time step

In the present article, to mitigate the influence of time delay on structure control, a genetic algorithm and two kinds of ANN were used for semi-active control of structures equipped with MR dampers. The data required for ANN training is generated using a GA. When the structure is subjected to the El-Centro earthquake, the GA is executed at each time step to minimize the structure’s maximum drift. Optimization variables are the force required to control the structure. Using the force obtained by the GA and the dampers' velocity, the required voltage for the dampers can be calculated using the dampers' inverse model. The ANN's input is composed of structural responses at each time step. The voltage required by the dampers in the next step forms the ANN's output. Three benchmark structures are used to evaluate the efficiency of the proposed methodology. Each structure is evaluated twice with a different number of dampers to determine the effect of increasing dampers on the structure's control.

This article is divided into four sections. The introduction is presented first. The second section describes the applied algorithms and analysis methods. In section 3, six numerical examples are analyzed, and the results of seismic responses of several structures controlled by the proposed methodology are presented. Section 4 concluded the paper.

2. METHODOLOGY

The control force of the MR damper depends on the input voltage and the difference of velocity at its two ends. The damper's behavior can be controlled by changing the input voltage. In this research, the back-propagation ANN is used to predict the required voltage of the dampers. Fig. 1 depicts the control process diagram.

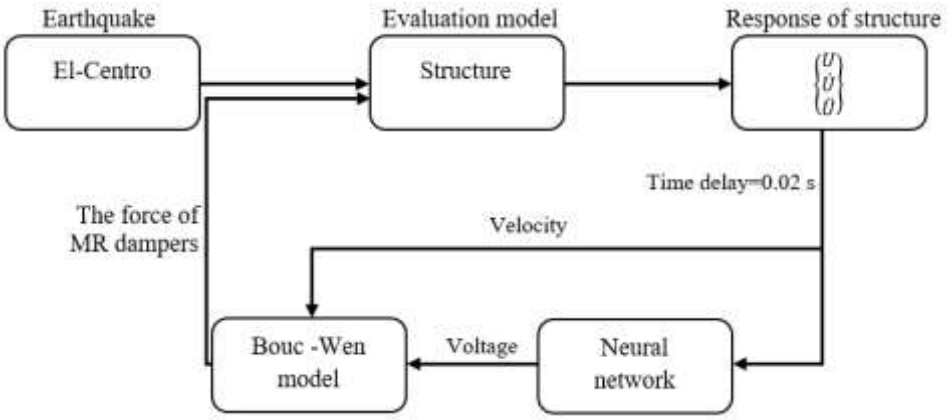

Figure 1. The flow of the semi-active control structure

The accelerogram of the El-Centro earthquake is used to obtain the training data. For this purpose, the structure is subjected to the El-Centro earthquake, and the required control force is calculated by the GA. It is assumed that the acceleration in the current step of analysis is available. Although this value is not available when the earthquake occurs, this assumption is made to provide the training data. For example, if the structure is equipped with two dampers, two control forces in each time step are calculated by the GA. Subsequently, using the damper force and the relative velocity of both ends at each time step, the required voltage is obtained from the inverse model of the damper. The inverse model is a lattice neural network. The damper's speed and force as inputs, this neural network can predict the corresponding damper's voltage. Therefore, the previous time step's seismic responses of the structure and the current time step's corresponding voltage of the MR dampers are available. By inputting structural responses, the multi-layer perceptron neural network is trained to predict the corresponding voltage of the dampers. Fig. 2 shows the flow of the semi-active control structure.

Fast learning and convergence to the optimal regression surface are two main advantages of GRNN when the number of samples is very high [37]. GRNN is especially useful in modelling sparse data in a real-time environment.

The GRNN can be regarded as a normalized radial basis function (RBF) network in which there is a remote unit concentrated on each training example [38]. This neural network is a one-pass learning algorithm with a parallel structure, and this feature results in the high speed of the neural network. Fig. 3 shows a schematic pattern of the neural network.

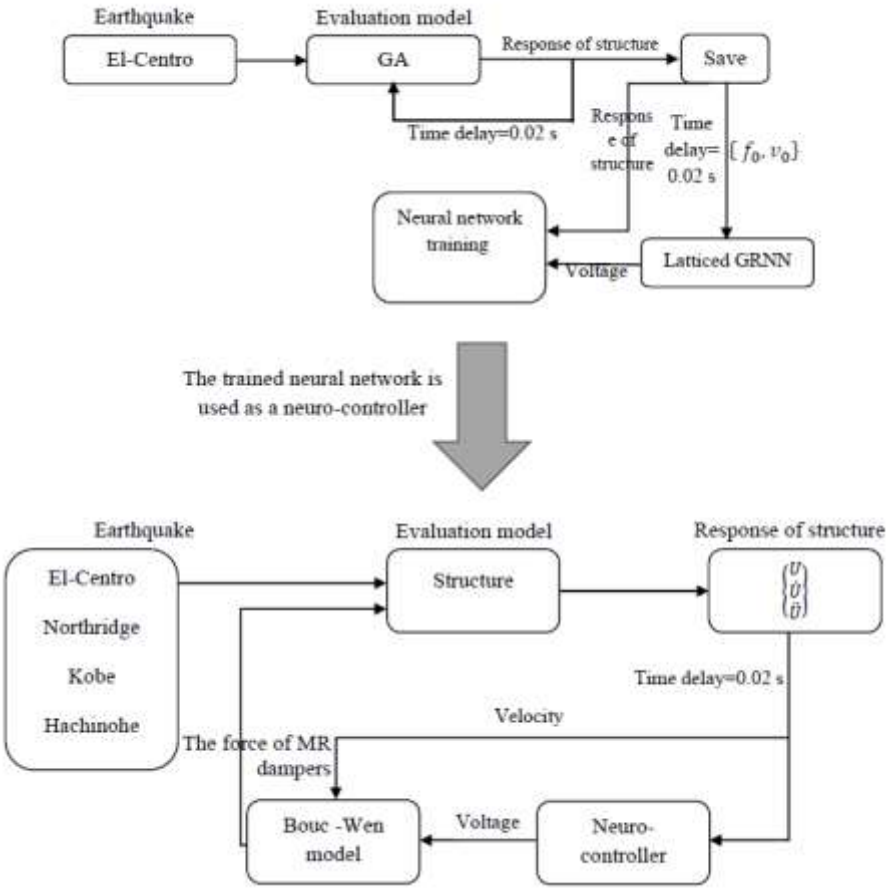

Figure 2. The flow of the semi-active control structure and the ANN training

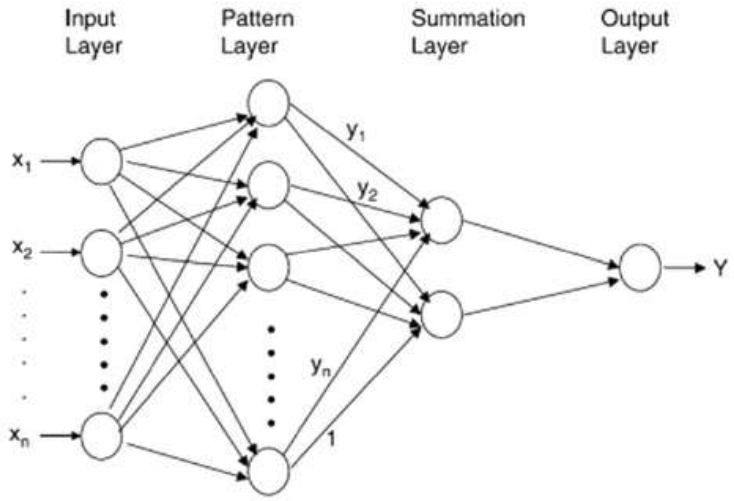

Figure 3. A schematic pattern of the GRNN architecture

The input units are in the first layer; the pattern units are in the second layer; in the third layer, the outputs of this layer are passed on to the summation units, and the output units are in the final layer. In the first layer, the number of neurons is the same as the number of attributes. The first-layer weights are adjusted to the transpose of the input vector, and the bias b is adjusted to the column vector of $0.8326/\sigma$. The smoothness parameter σ is selected by the user. The second layer also has as many neurons as input vectors. The hidden-to-output weights are just the response values; hence, the output is defined as a weighted average of the target values of the training cases close to the assumed input case, based on the weights corresponding to the Euclidean distances between the training input vectors and the test input vector.

$$\hat{y}(x) = E(y|x) = \frac{\sum_{i=1}^{n} y_i h_i}{h_i}, \quad h_i = \exp\left(-\frac{d_i^2}{2\sigma_i^2}\right) d_i^2 = (x - x_i)^T (x - x_i) \tag{1}$$

where the Gaussian radial basis function is shown by h_i, the smoothing parameter is shown by s, and d_i^2 denotes the squared euclidean distance between a test input vector x and x_i.

2.1 Genetic algorithm

The GA used in this article obtains the force of each damper to minimize the maximum drift of the structure. Therefore, the number of optimization variables is equal to the number of dampers in the control structure. Hence, the size of the population members depends on the number of dampers used in the control structure. In the numerical examples, the number of dampers changes. For this reason, the GA used is described in all numerical examples. The values of crossover fraction and function tolerance are 0.8 and10^{-6}, respectively. In using the GA to determine the proper damper force, it is assumed that the earthquake acceleration in the following step is known. The Newmark-Beta method is used for the dynamic analysis of the structure. The fitness function of the GA is obtained by solving the equations from a time step. The structural responses at the previous step form the initial conditions for the current step. Fig. 4 shows the calculation of the force of dampers by the GA.

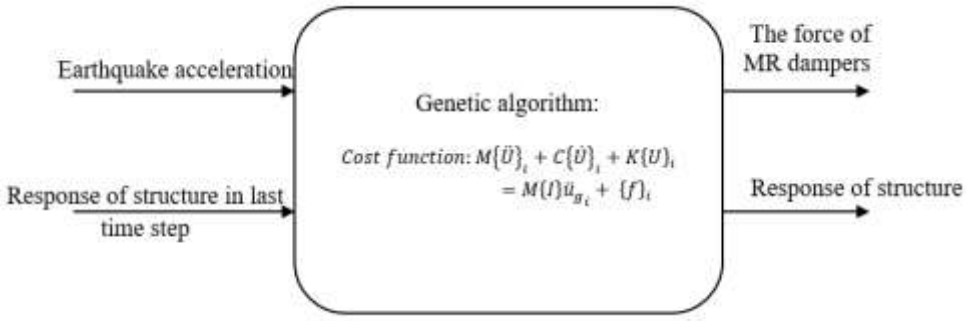

Figure 4. A schematic diagram of the way the control force is calculated by GA

In Fig. 4, the displacement, velocity, and acceleration of the structure in time step i are represented by $\{U\}$, $\{\dot{U}\}$ and$\{\ddot{U}\}$, respectively. In addition, $\{f\}_i$ and $\ddot{U}_{g_i}$ represents the

earthquake's acceleration. The structural responses and the optimal control force of dampers were saved after all steps of the earthquake were analyzed, and subsequently they were utilized to simulate the inverse behavior of dampers in the next step.

2.2 Simulation of the inverse behavior of dampers with GRNN

GRNN calculates the corresponding voltage using the damper force and velocity of the structural stories as input variables. By obtaining the difference of the velocity in the stories in which the ends of the dampers are located, the relative velocity of both ends of the damper is calculated. The Bouc-wen mathematical model is then used to simulate the behavior of the damper. The equations are defined as follows[32].

$$f = c_0\dot{x} + \alpha z \tag{2}$$
$$\dot{z} = -\gamma|\dot{x}|z|z|^{n-1} - \beta\dot{x}|z|^n + A\dot{x} \tag{3}$$
$$\alpha = \alpha_a + \alpha_b u \tag{4}$$
$$c_0 = c_{0a} + c_{0b} u \tag{5}$$

The parameters' values are given as follows.

$$\alpha_a = 1.0872e2\ \frac{N}{cm} \tag{6}$$
$$\alpha_b = 4.9616e5\ \frac{N}{cm.V} \tag{7}$$
$$C_{0a} = 4.40\frac{N.s}{cm} \tag{8}$$
$$C_{.b} = 44.0\frac{N.s}{cm.V} \tag{9}$$
$$\eta = 50s^{-1} \tag{10}$$
$$\gamma = 3\ cm^{-1} \tag{11}$$
$$\beta = 3\ cm^{-1} \tag{12}$$
$$A = 1.2 \tag{13}$$

The steps of the voltage are considered to be 0.1 volts. If higher accuracy is required, this value can be decreased, but the cost of computations also increases. As it was mentioned in the previous section, the control force of the damper was computed by the GA. By performing the time history analysis, the structural responses are also obtained. As the velocity and force of the MR damper are now available. Using GRNN as described in the following model, the corresponding voltage can be calculated.

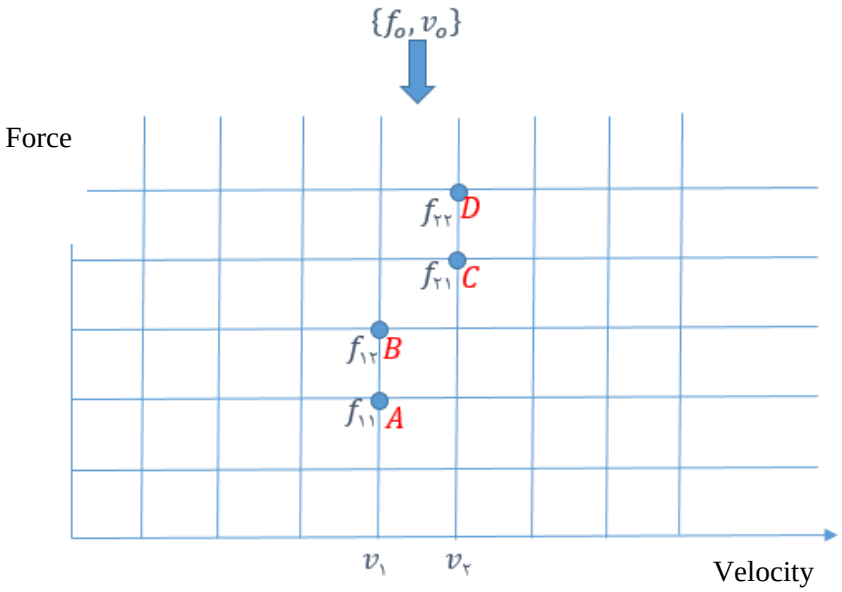

Figure 5. The way the closest points to the point of interest are found to train the GRNN

As shown in Fig. 5, the velocity and the corresponding force are inputs of latticed GRNN. V_0 and f_0 are the velocity and the corresponding force, respectively. First, the closest value to v_0 is obtained. In other words, v_0 value is limited to two values in the network. These two values are denoted by $v_1$and v_2. Then, this is done for the force corresponding to these values. The values are determined by f_{11}, f_{21}, f_{12} and f_{22} in Fig. 5. Now, four points with the least distance to the input point, (v_0, f_0), are determined.

In this step, the goal is to obtain the voltage corresponding to the points v_0 and f_0. GRNN is used to calculate the voltage corresponding to the input point regarding these four points. The training data are the coordinates of four points A, B, C, and D. A GRNN is trained by coordinates of force and velocity of the points and the target data is the third coordinate of the points or the equivalent voltage. After training, the network can predict the voltage corresponding to the data of the force and velocity(v_0, f_0).

2.3 Prediction of the dampers' voltage

Thus far, the structural responses and optimal control forces, as well as the voltage corresponding to the force, have been determined in accordance with the earthquake's acceleration at each time step. The multi-layer ANN is subsequently used to predict the appropriate voltage using these values. The network's architecture varies according to the number of inputs and outputs. As a result, the network architecture that is most appropriate for each numerical case is selected. There are one or two hidden layers in the networks. The layer's total number of neurons is determined by analyzing ANNs for each numerical example. Each network is run multiple times and the ANN having the best performance is used to evaluate the network's efficiency. The network's input consists of the displacement, velocity, and acceleration of the stories, as well as the velocity of dampers. For example, in a numerical example involving a three-story structure, the input vector contains twelve

components. The output of the network is the voltage of the dampers; thus, in a three-story structure, this vector has three components.

2.4 Dynamic analysis of the structure

The differential equation governing the motion of the structure was solved using the Newmark-β formulation. At each time step, these equations are solved. Following the calculation of structural responses at each step, the control force can be calculated. In 1959, Newmark introduced the following equations as a class of time step formulations [39].

$$\dot{u}_{j+1} = \dot{u}_j + [(1-\gamma)\Delta t]\ddot{u}_j + (\gamma \Delta t)\ddot{u}_{j+1} \tag{14}$$

$$u_{j+1} = u_j + \Delta t\dot{u}_j + [(0.5-\beta)\Delta t^2]\ddot{u}_j + (\beta \Delta t^2)\ddot{u}_{j+1} \tag{15}$$

In these equations, $\ddot{u}_{j+1}$, u_{j+1} and $\dot{u}_{j+1}$ are the acceleration, displacement, and velocity of the stories of the structure, respectively. The constant length of the time interval is denoted by Δt. The factors γ and β denote the variations of the acceleration at each time step, and the stability and accuracy of the formulation. The values 1/2 and 1/6 are used for γ and β, assuming linear variations of the acceleration at each time step. The equations (14), (15), and the motion equation of the structure at the end of the time step are used to calculate u_{j+1}, $\dot{u}_{j+1}$ and $\ddot{u}_{j+1}$ at the time i+1 from u_j, $\dot{u}_j$ and $\ddot{u}_j$. Iterations are required to complete the analysis because $\ddot{u}_{j+1}$ is in the right-hand side of the equations (14) and (15). In this article, the behavior of the frame is assumed to be linear. In the linear systems, the Newmark formulation can be simplified by using parameter differences instead of their values in time steps. This is performed by changing the quantities as follows.

$$\Delta u_i = u_{i+1} - u_i \tag{16}$$

$$\Delta \dot{u}_i = \dot{u}_{i+1} - \dot{u}_i \tag{17}$$

$$\Delta \ddot{u}_i = \ddot{u}_{i+1} - \ddot{u}_i \tag{18}$$

$$\Delta p_i = p_{i+1} - p_i \tag{19}$$

In the above equations, Δu_i is the change in displacement, $\Delta \dot{u}_i$ is the change in velocity, $\Delta \ddot{u}_i$ is the change in acceleration, and Δp_i is the change in force at i-th time step. By using the formulations, the equations (14) and (15) and the motion equation of the structure can be rewritten as follows.

$$\Delta \ddot{u}_i = \left(\frac{1}{\beta(\Delta t)^2}\right)\Delta u_i - \left(\frac{1}{\beta \Delta t}\right)\dot{u}_i - \left(\frac{1}{2\beta}\right)\ddot{u}_i \tag{20}$$

$$\Delta \dot{u}_\iota = \left(\frac{\gamma}{\beta \Delta t}\right)\Delta u_i - \left(\frac{\gamma}{\beta}\right)\dot{u}_i - \Delta t\left(1 - \frac{\gamma}{2\beta}\right)\ddot{u}_i \tag{21}$$

$$m\Delta \ddot{u}_i + c\Delta \dot{u}_i + k\Delta u_i = \Delta p_i \tag{22}$$

The changes in structural responses are determined by employing these equations at each time step. By using the structural responses at the beginning of the time step, the values at the end of the step are calculated.

2.5 Evaluation indices

In the numerical examples investigated in the next section, the structure is controlled with a different number of dampers. To measure the performance of the proposed control mechanism, the following performance indices are used [40].

$$J_1 = max\left\{\frac{max_{t,i}\left|{d_i(t)}/{h_i}\right|}{\sigma_{max}}\right\} \tag{23}$$

$$J_2 = max\left\{\frac{max_{t,i}|\ddot{x}_{ai}(t)|}{\ddot{x}_{max}}\right\} \tag{24}$$

The index J_1 is related to the maximum drift of the stories. In the equation (23), $d_i(t)$ denotes the internal relative displacement of the structure and σ_{max} is its maximum value in the uncontrolled state. J_2 index is related to the maximum acceleration. The parameters $\ddot{x}_{ai}$ and $\ddot{x}_{max}$ are the acceleration of the i-th story at each time step in the controlled state and the maximum acceleration in the uncontrolled state, respectively. It should be noted that the GA is employed to minimize the performance index J_1 when the structures are exposed to the El-Centro earthquake.

3. NUMERICAL EXAMPLES

In this section, three−, eleven- and twenty-story structures are examined with a different number of dampers. In each numerical example, the features of the structure are stated. Moreover, appropriate charts and tables are presented to demonstrate the efficiency of the presented methodology.

3.1 The first numerical example

This numerical example examines the efficiency of the proposed methodology to control a three-story structure. The mass of each story is 4×10^5 kg, and its stiffness is 1.6×10^8 N/m [41]. Four dampers are installed in the structure. Two dampers are placed in the first story, and one damper is placed in other stories. The damping matrix of the structure was obtained by the Rayleigh method so that the damping of the first and second vibration modes of the structure is 5%. First, the force of each damper is computed by the acceleration in the next step using the GA. This was done for data of the El-Centro earthquake. The plot of the control force of the damper in the third-story is depicted in Fig. 6. The plot corresponds to the first 8 seconds of the El-Centro earthquake.

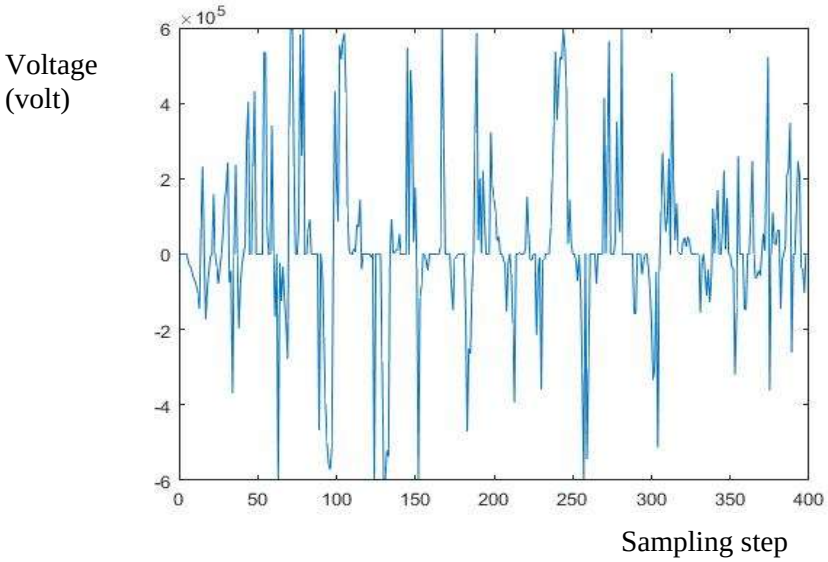

Figure 6. The required control force of the damper in the third-storey

The time interval of the sampling is 0.02 s. By using the required control force and the velocity of the structure's stories, the voltage of the dampers is obtained at each time step by the proposed methodology. The voltage-time plot of the damper in the third-story is presented in Fig. 7.

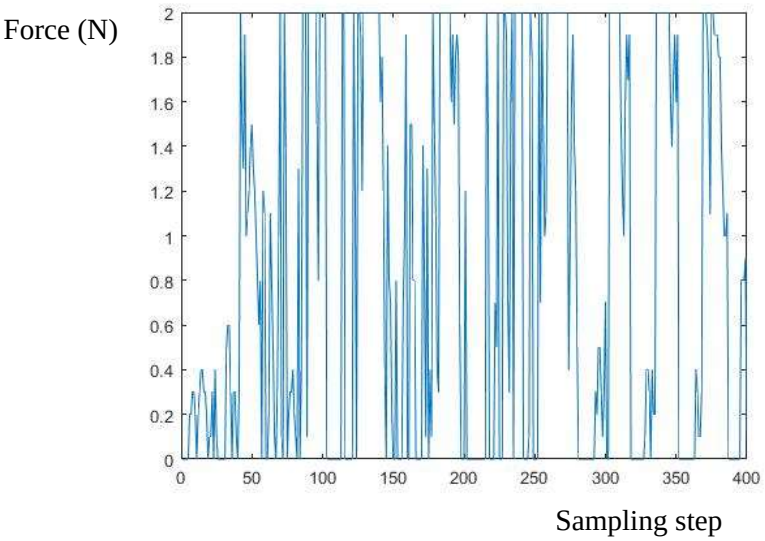

Figure 7. Required voltage of the damper in the third-story

3.1.1 ANN predicting the voltage

The ANN is used to predict the voltage. The ANN's input is the structural responses, and its output is the dampers' voltage in the next step. The voltages required for two dampers in the

first story are assumed to be equal. Therefore, the output of the ANN is a vector with three components. Displacements, velocities, acceleration, and velocity of dampers are used as the input of the ANN and therefore, the input vector has twelve components. Two thousand four hundred data of the El-Centro earthquake and the equivalent structural responses are used to train and test the ANNs. Seventy percent of these data are used for training the ANN, and the remaining data is used for testing the ANN. In Fig. 8, the actual and predicted values of the voltage of the third-story damper are compared.

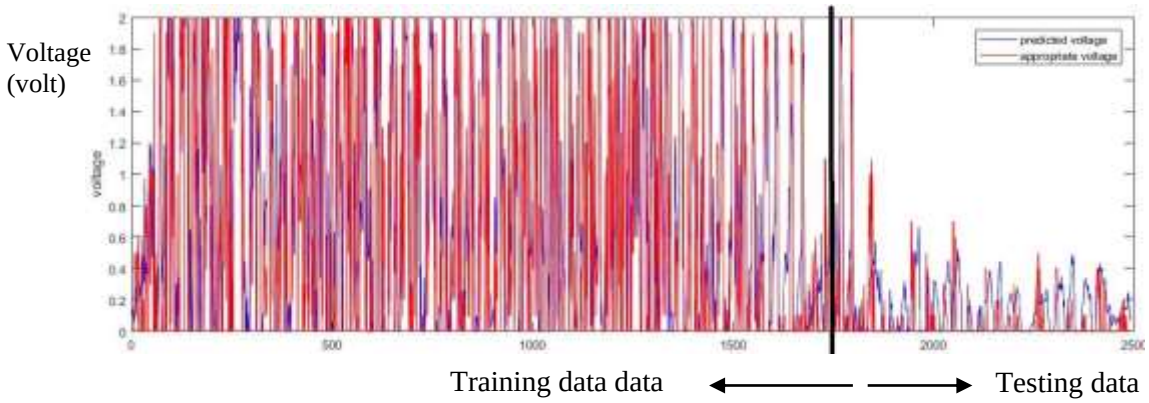

Figure 8. Comparison of the predicted voltage and the required voltage of the damper in the third-story

Eighteen different ANNs are examined with different number of layers and neurons to achieve the best results. Table 1 presents the means squared errors and the number of neurons in the hidden layer of the corresponding ANN. The results related to six ANNs having the best performance are shown in Table 1. It should be mentioned that each ANN is trained fifteen times.

Table 1: Architecture and error of ANNs

Number of neurons in the hidden layer	Mean squared error in ten training and testing NN			
	Training		Testing	
	Average	Best	Average	Best
15	0.2031	0.1732	0.1441	0.0827
20	**0.2003**	**0.1587**	**0.1458**	**0.0598**
25	0.2006	0.1706	0.1572	0.0932
30	0.2026	0.1771	0.1646	0.1120
35	0.2059	0.1629	0.1728	0.1084

Due to the importance of the ANN prediction in the presented methodology, an ANN is used in the control structure that has the best performance to predict the voltage. Results presented in table 1, indicate that an ANN with 20 neurons in the hidden layer has the best performance. Therefore, this ANN is used in the control structure.

3.1.2 Semi-active controller

After training the ANN, the ANN is used to predict the voltage of the dampers in the current step by using the structural responses in the previous step. It is emphasized that the training data of the ANN were obtained when the structure was subjected to the El-Centro earthquake. For this reason, other earthquakes such as Northridge, Hachinohe, and Kobe are also used to test the efficiency of the proposed methodology. Two criteria related to drift and absolute acceleration described in section 2.6 are used for evaluating the efficiency of the proposed methodology.

Table 2: The performance indices when the structure is excited by several earthquakes

Earthquake	J1	J2
El-Centro	0.9143	0.9297
Kobe	0.8695	0.8797
Hachinohe	0.6576	0.7919
Northridge	0.9099	0.9493
Average of four earthquakes	0.8378	0.8876

As shown in Table 2, the proposed control method can control the structure's behavior and reduce the drifts and accelerations. Although the data of the El-Centro earthquake is used to prepare the training data of the ANN, the proposed control method has also been effective when the structure is excited by other earthquakes. On average, the presented method has reduced the drift criterion to 16.22%. It should be noted that although the training data were obtained to reduce the maximum drift of the stories, acceleration has also been decreased.

3.2 The second numerical sample

In the second example, the three-story structure of the first numerical example is reexamined. In this example, six dampers are used to control the structure's responses. In other words, the effect of the increase in the control power will be examined on the behavior of the previous structure. Two dampers are placed in each story of the structure. Damping of the first two modes of the structure is 5% that is the calculated Rayleigh method. The structural control process is the same as the first numerical example. The force calculated using the GA for controlling the structure's responses is equal to the value calculated in the numerical example. The only difference is that the force must be provided at each story with two dampers. The purpose of the numerical example is to use a more significant control force to control the structure's behavior. The diagram of the voltage of the damper in the third-story is presented in Fig. 9. This figure shows the voltage of a damper. The voltage of the second damper is also equal to this value because the force of the dampers is the same at each story.

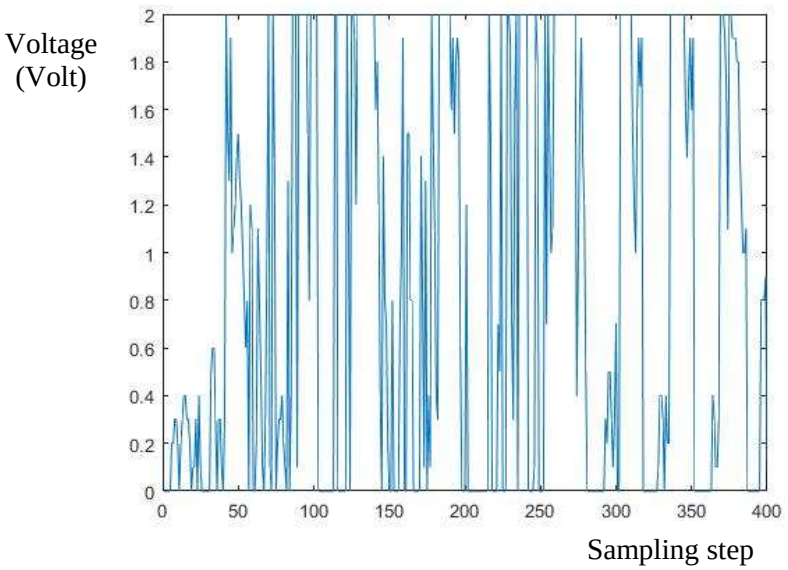

Figure 9. The voltage of the damper at the roof in the first 8 seconds of El-Centro earthquake

According to the plot presented in Fig. 9, it is noted that the damper works with its maximum power at certain times. Hence, it is deducted that using two dampers may be more useful in the story. The architecture of the ANN, the input and output data, are the same as the first numerical example. The ANN in the control structure and the evaluation indices of the structure under the effect of the El-Centro, Northridge, Kobe, and Hachinohe earthquakes are presented in Table 3.

Table 3: The performance indices when the structure is excited by several earthquakes

Earthquake	J1	J2
El-Centro	0.8695	0.8891
Kobe	0.8411	0.8275
Hachinohe	0.6010	0.7644
Northridge	0.9179	0.9268
Average of four earthquakes	0.8065	0.8645

Comparing the results of the first and second examples, it can be noted that the average index of the maximum drift of the stories in the second example is about 3% more than the equivalent value in the first numerical example. Also, the index of the maximum acceleration of the stories has decreased up to 2%.

3.3 The third numerical example

In this numerical example, an eleven-story structure is used. Mass and stiffness of each story of the structure are given in Table 4. Damping of the structure is obtained by the Rayleigh method so that damping of the first and second modes of the structure is 2% [22]. The natural period of the structure is 0.86 seconds.

Table 4: Mass and stiffness of the structure's stories

Number of stories	Mass of story (Kg)	Stiffness of the structure's stories (KN/m)
1	4.68×10^5	215370
2	4.76×10^5	201750
3	4.5×10^5	201750
4	4.5×10^5	200930
5	4.5×10^5	200930
6	4.5×10^5	200930
7	4.37×10^5	203180
8	4.37×10^5	202910
9	4.37×10^5	202910
10	4.37×10^5	176100
11	3.12×10^5	66230

In this numerical example, a damper is used in all stories of the structure. The ANN used in the control structure is the same as the previous numerical examples, i.e., it is the multi-layer perceptron neural network. The ANN has 44 neurons in the input layer. The voltage of the damper in each story is in the output layer. Therefore, the output layer has 11 neurons. Several ANNs with different number of neurons in hidden layers are investigated to obtain the best architecture. The mean squared error of training and testing data in ten different runs of ANNs is presented in Table 5.

Table 5: Number of neurons in the hidden layers and mean squared error of ANNs

Number of neurons in the hidden layers	Mean squared error in ten training and testing ANNs			
	Training		Testing	
	Average	Best	Average	Best
11-11	0.1696	0.1571	0.0475	0.0419
15-11	0.1704	0.1570	0.0499	0.0401
15-14	0.1629	0.01401	0.0486	0.0352
16-12	0.1698	0.1452	0.0513	0.0367
20-11	**0.1660**	**0.1349**	**0.0501**	**0.0358**

According to the results presented in Table 5, it can be seen that an ANN with 20-11 neurons in the first and second hidden layers has a good performance in predicting voltage. Hence, this ANN is used in the control structure. The evaluation indices are presented in Table 6.

Table 6: The performance indices when the structure is excited by several earthquakes

Earthquake	J1	J2
El-Centro	0.5823	0.8548
Kobe	0.7610	0.9294
Hachinohe	0.5740	0.7359
Northridge	0.8081	0.9381
Average of four earthquakes	0.6813	0.8645

The proposed method has been very effective as the maximum drift of the structure has been decreased. It can be observed that J1 has decreased in all earthquakes. The average value of the indices of drift and acceleration is 0.6813 and 0.8645, respectively, demonstrating an acceptable reduction in the displacements and accelerations using the proposed methodology.

3.4 The fourth numerical example

In this numerical example, an eleven-story structure is selected again whose features are examined in the previous example, but the number of dampers is different from the third example. In the same manner as previous examples, the required force of dampers is obtained by the GA to reduce the relative displacement of the structure. The number of optimization variables is equal to the number of degrees of freedom of the structure. The population size is set at 40, and data recorded in the El-Centro earthquake is used. To control the structure, two dampers are placed in the stories one to ten, and one damper is placed in the eleventh story. Features of the damper are similar to the previous numerical example. The performance indices are given in Table 7 for the El-Centro, Northridge, Kobe, and Hachinohe earthquakes.

Table 7: The performance indices when the structure is excited by several earthquakes

Earthquake	J1	J2
El-Centro	0.4135	0.8489
Kobe	0.6976	0.9365
Hachinohe	0.4096	0.8351
Northridge	0.8012	0.9080
Average of four earthquakes	0.5805	0.8821

By comparing the results presented in Tables 6 and 7, it can be noted that as the number of dampers increases, the system's ability to control the structural responses also increases.

3.5 The fifth numerical example

This numerical example considers twenty-story benchmarks equipped with dampers. Two dampers are used in the first and second stories, and one damper is placed on the other floors. The seismic mass of the first floor is one, the seismic mass of the second to nineteenth floors is two, and the seismic mass of the structure's roof floor is three. The number of optimization variables equals the number of forces applied to the structure by the dampers, which is 20 in this example. The population size of GA is set as five times the number of variables and equal to 100. The GA determines the appropriate damper force to reduce the structure's maximum drift under the impact of the El-Centro earthquake. After examining ANNs with varying numbers of neurons are examined and the optimal ANN is chosen to be used as a controller. Due to the random selection of ANN weights, each ANN was evaluated ten times and the best ANN was then selected. Table 8 displays the mean squared error of each ANN for training and testing data. An ANN with 80-40 neurons in the first and second hidden layers has the best performance and is selected as the controller.

Table 8: The performance indices when the structure is excited by several earthquakes

Number of neurons in the hidden layer	Mean squared error in ten training and testing NNs			
	Training		Testing	
	Average	Best	Average	Best
70-30	0.1324	0.0128	0.0588	0.0425
75-30	0.1560	0.1445	0.0574	0.0506
75-38	0.1567	0.1444	0.0603	0.0485
80-40	**0.1324**	**0. 1280**	**0.0588**	**0.0425**
80-45	0.1562	0.1335	0.0620	0.0444

The controller composed of the selected ANN is assessed under the influence of the El-Centro, Kobe, Northridge, and Hachinohe earthquakes. The criteria of maximum acceleration and maximum drift are listed in Table 9.

Table 9: The performance indices when the structure is excited by several earthquakes

Earthquake	J1	J2
El-Centro	0.6296	2.5279
Kobe	0.7978	1.0145
Hachinohe	0.7284	0.9404
Northridge	0.9865	۰/۹۹۶۵
Average of four earthquakes	0.7855	1.3697

El-Centro and Hachinohe earthquakes are far-fault and Northridge and Kobe earthquakes are near-fault. As demonstrated by the presented data in Table 9, the presented method is more efficient in far-faults earthquakes (El-Centro and Hachinohe).

3.6 The sixth numerical example

In this example, two dampers are placed on the first to fifth floors and one damper is placed on the other stories. This structure is controlled by the same ANN used in the fifth example. Table 10 illustrates the control criteria when the structure is subjected to multiple earthquakes.

Table 10: The performance indices when the structure is excited by several earthquakes

Earthquake	J1	J2
El-Centro	0.66.6	10.496
Kobe	0.7481	0.9909
Hachinohe	0.6377	1.2769
Northridge	0.9048	1.035
Average of four earthquakes	0.7378	1.0881

Criteria J_1 and J_2 presented in table 10 make the comparison between the controlled and uncontrolled structures. Table 11 compares the results of the controlled structure for 20-story structure with the results published in Ohtori et al. [40]. This table displays the results of two numerical examples (fifth and sixth examples), as well as the results of Ohtori et al. [40].

Table 11: Comparison the method described in Ohtori et al. [40] with the neural controllers used in this article

Earthquake		J_1	J_2
El-Centro	1	0.6296	2.5279
	2	0.6606	1.0496
	3 [40]	0.748	0.646
Kobe	1	0.7978	1.0145
	2	0.7481	0.9909
	3 [40]	0.728	0.839
Hachinohe	1	0.7284	0.9404
	2	0.6377	2769
	3 [40]	0.887	0.743
Northridge	1	0.9865	0.9965
	2	0.9048	1.035
	3 [40]	0.942	0.904

The numbers 1, 2, and 3 in this table denote the fifth numerical example, the sixth numerical example, and the results published by Ohtori et. al [40]. These results demonstrate that the proposed control methodology significantly reduces structural seismic responses. The displacement of the structure's roof during the El-Centro and Kobe earthquakes is depicted in Fig. 10 in the controlled and uncontrolled states.

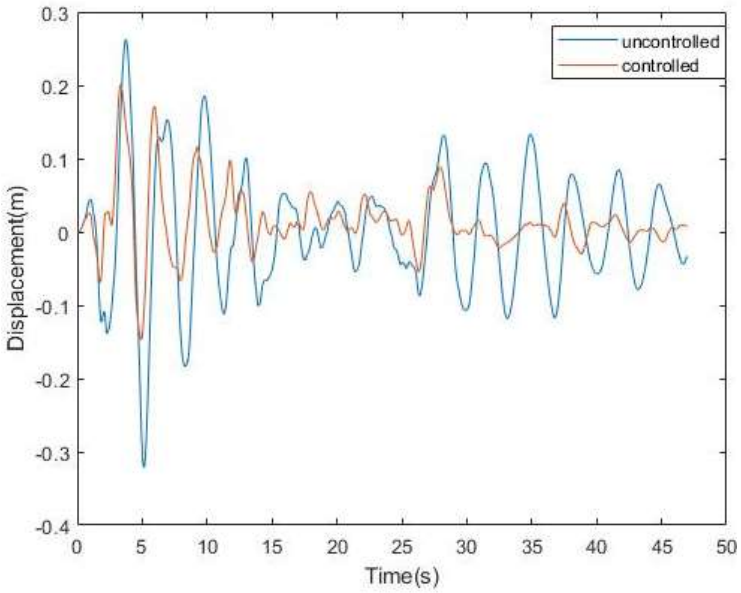

Figure 10. Roof displacement during the El-Centro earthquake as a result of the dampers distribution used in the sixth numerical sample

4. CONCLUSION

In this article, a methodology using the genetic algorithm and two different kinds of ANNs was proposed for semi-active control of structures equipped with MR dampers. Six numerical examples of three- story, eleven- story, and twenty-story structures were used to demonstrate the efficiency of the proposed methodology., The proposed neuro-controller is trained to predict the required voltage for the MR dampers by receiving the responses from the previous earthquake step. As the amount of damage to the structure is proportional to the maximum drift of structure, the objective function of the genetic algorithm in all provided examples is defined as minimizing the maximum drift. As the Genetic algorithm is used to obtain the data required for ANN training with the objective of minimizing the maximum structural drift at each earthquake time step, the preparation of training data is time-consuming. However, it should be noted that as this step is included in the process of preparing the controller, it has no adverse effect on the structural control process.

The results of six numerical examples demonstrated a significant reduction in the maximum drift in the controlled state of all structures.The results of the twenty-story structure were compared with previously published results [40]. These results shows that the rate of reduction in the maximum drift of the structure in Hachinohe and El-Centro earthquakes is 36.23 and 33.94 percent, respectively. This value is equal to 26.19 and 9.52 percent in Kobe and Northridge earthquakes, respectively.

REFERENCES

1. Roy T, Matsagar V Probabilistic assessment of steel buildings installed with passive control devices under multi-hazard scenario of earthquake and wind, *Struct Safe* 2020; **85**: 101955. doi: 10.1016/j.strusafe.2020.101955.
2. Roësset JM,. Yao JTP. State of the art of structural engineering, *Perspectives in Civil Engineering: Commemorating the 150th Anniversary of the American Society of Civil Engineers*, pp. 131–141, 2003, doi: 10.1061/(asce)0733-9445(2002)128:8(965).
3. Kaveh A. Statistical seismic performance assessment of tuned mass damper inerter, *Struct Contr Health Monitor,* 5th July, 2020: 1–24. doi: 10.1002/stc.2602.
4. Abbasi M, Markazi AHD. Optimal assignment of seismic vibration control actuators using genetic algorithm, *Int J Civil Eng* 2014, **12**(1): 24–31. doi: ijce.iust.ac.ir/article-1-647-en.html.
5. Rezaiee-Pajand M, Payandeh-Sani M. Three schemes for active control of the planner frame, *International J Optim Civil Eng* 2015, **5**(1): 117-35.
6. Bhaiya V, Bharti SD, Shrimali MK, Datta TK. Genetic algorithm based optimum semi-active control of building frames using limited number of magneto-rheological dampers and sensors, *J Dyn Syst, Measurem, Contr* 2018; **140**: 1–13. doi: 10.1115/1.4040213.
7. Agrawal AK, Yang JN. Semi-active hybrid control systems for nonlinear buildings against near-field earthquakes, *Eng Struct* 2002, **24**(3): 271-80.
8. Xu YL, Chen J, Ng CL, Qu WL. Semiactive seismic response control of buildings with podium structure, *J Struct Eng* 2005; **131**(6): 890-9. doi: 10.1061/(asce)0733-9445(2005)131:6(890).

9. Dominguez A, Sedaghati R, Stiharu I. Modeling and application of MR dampers in semi-adaptive structures, *Comput Sruct* 2008, **86**(3–5): 407–415. Feb., doi:10.1016/j.compstruc. 2007.02.010.
10. Butz T, Von Stryk O. Modelling and simulation of electro - and magnetorheological fluid dampers, *ZAMM Zeitschrift fuer Angewandte Mathematik und Mechanik* 2002, **82**(1): 3–20. doi: 10.1002/1521-4001(200201)82:1.
11. Dyke SJ, Spencer Jr BF, Sain MK, Carlson JD. Modeling and control of magnetorheological dampers for seismic response reduction, *Smart Mater Struct Model* 1996; **5**: 565-75.
12. Wang N, Adeli H. Self-constructing wavelet neural network algorithm for nonlinear control of large structures, *Eng Applicat Artific Intell* 2015; **41**: 249–58. doi: 10.1016/j.engappai .2015.01.018.
13. Miyamoto K, Sato D, She J. A new performance index of LQR for combination of passive base isolation and active structural control, *Eng Struct* 2017; **157**: 280-99. doi: 10.1016/j.engstruct.2017.11.070.
14. Bani-hani KA, Sheban MA. Semi-active neuro-control for base-isolation system using magnetorheological (MR) dampers, *Earthq Eng Struct Dyn* 2006: 1119-44. doi: 10.1002/eqe.574.
15. Allaoua S, Guenfaf L. LQG vibration control effectiveness of an electric active mass damper considering soil – structure interaction, *Int J Dyn Contr* 2018. doi: 10.1007/s40435-018-0428-9.
16. Chase JG, Smith HA, Suzuki T. Robust H∞ control considering actuator saturation. II: applications, *J Eng Mech* 1996; **122**(10): 984-93. doi: 10.1061/(asce)0733-9399(1996)122:10(984).
17. Wang A, Lee C. Fuzzy sliding mode control for a building structure based on genetic algorithms, *Earthq Eng Struct Dyn* 2002; 895: 881-95. doi: 10.1002/eqe.127.
18. Laflamme S, Slotine JJE, Connor JJ. Wavelet network for semi-active control, *J Eng Mech* 2011; **137**(7): 462-74. doi: 10.1061/(asce)em.1943-7889.0000248.
19. Khaje-Karamodin A, Haji-Kazemi H, Rowhanimanesh AR, Akbarzadeh-Tootoonchi MR. Semi-active control of structures using a neuro-inverse model of MR dampers, *Sci Iran* 2009; **16**(3): 256-63. doi: 10.1061/(ASCE)0733-9399(2000)126:8(795).
20. Gu X, Yu Y, Li Y, Li J, Askari M, Samali B. Experimental study of semi-active magnetorheological elastomer base isolation system using optimal neuro fuzzy logic control, *Mech Syst Signal Process* 2019; **119**: 380–398. doi: 10.1016/j.ymssp.2018.10.001.
21. Fallah AY, Taghikhany T. Robust semi-active control for uncertain structures and smart dampers, *Smart Mater Struct* 2014; **23**(9). doi: 10.1088/0964-1726/23/9/095040.
22. Bathaei A, Zahrai SM, Ramezani M. Semi-active seismic control of an 11-DOF building model with TMD þ MR damper using type-1 and -2 fuzzy algorithms, *J Vib Contr* 2016. doi: 10.1177/1077546317696369.
23. Kim DH, Kim D, Chang S, Jung HY. Active control strategy of structures based on lattice type probabilistic neural network, *Probabil Eng Mech* 2008; **23**(1): 45–50. doi: 10.1016/j.probengmech.2007.10.004.
24. Vadtala IH, Soni DP, Panchal DG. Semi-active control of a benchmark building using neuro-inverse dynamics of MR damper, *Proced Eng* 2013; **51**: 45-54. doi: 10.1016/j.proeng.2013.01.010.
25. Kaveh A, Gholipour Y, Rahami H. Optimal design of transmission towers using genetic algorithm and neural networks, *Int J Space Struct* 2008; 23(1): 1–19. doi:10.1260/ 026635108785342073.

26. Kaveh A, Iranmanesh A. Comparative Study of backpropagation and improved counterpropagation neural nets in structural analysis and optimization, *Int J Space Struct* 1998, **13**(4): 177–85. doi: 10.1177/026635119801300401.
27. Kaveh A, Khalegi A. Prediction of strength for concrete specimens using artificial neural networks, *Asian J Civil Eng* 2000; 2(2): 1–13. doi: 10.4203/ccp.53.4.3.
28. Kaveh A, Fazel-Dehkordi, Servati H. Prediction of moment-rotation characteristic for saddle-like connections using BP neural networks, *Asian J Cvil Eng* 2001; **1**(2): 11–30.
29. Nedushan B, Chouinard LE. Use of artificial neural networks for real time analysis of dam monitoring data, 2003.
30. Chouinard LE, Nedushan BA, Feknous N. Statistical analysis in real time of monitoring data for idukki arch dam.
31. Ghaboussi J, Joghataie A. Active control of strtuctures using nueral network, *Eng Mech* 1995; **121**(4): 555-67.
32. K-Karamodin A, H-Kazemi H. Semi-active control of structures using neuro-predictive algorithm for MR dampers, *Struct Control Health Monitor* 2010; **17**: 237-53.
33. Hashemi SMA, Kazemi HH, Karamodin A. Localized genetically optimized wavelet neural network for semi- active control of buildings subjected to earthquake, *Struct Control Health Monitor* 2016; **23**(8): 1074-7. doi: 10.1002/stc.
34. Bitaraf M, Ozbulut OE, Hurlebaus S, Barroso L. Application of semi-active control strategies for seismic protection of buildings with MR dampers, *Eng Struct* 2010; **32**(10): 3040-7. Oct., doi: 10.1016/j.engstruct.2010.05.023.
35. Zabihi-Samani M, Ghanooni-Bagha M. An optimal cuckoo search-fuzzy logic controller for optimal structural control, *Int J Optim Cvil Eng* 2018; 8(1): 117-35.
36. Katebi J, Mohammady Zadeh S. Time delay study for semi-active control of coupled adjacent structures using MR damper, *Struct Eng Mech* 2016; **57**(6): 1127-43.
37. Specht DF. General regression NN (GRNN), *Transact Neural Network* 1991; **2**(6): 568-76.
38. Ahmadi-Nedushan B. An optimized instance based learning algorithm for estimation of compressive strength of concrete, *Eng Applicat Artific Intell* 2012; 25(5): 1073-81. doi: 10.1016/j.engappai.2012.01.012.
39. Chopra AK. *Dyn of Structures*, Fourth, Prentice Hall, 2012.
40. Ohtori Y, Christenson RE, Spencer BF, Dyke SJ. Benchmark control problems for seismically excited nonlinear buildings, *J Eng Mech* 2004; **130**(4): 366-85. doi: 10.1061/(asce)0733-9399(2004)130:4(366).
41. Mortezaei A, Ronagh HR. Plastic hinge length of RC columns subjected to both far-fault and near-fault ground motions having forward directivity, *Struct Des Tall Special Build* 2014; **24**: 421-39. doi: 10.1002/tal.